

## Ice concentration and distribution near the south pole of Mars: Synthesis of odyssey and global surveyor analyses

R. L. Tokar, W. C. Feldman, T. H. Prettyman, K. R. Moore, D. J. Lawrence,  
and R. C. Elphic

Los Alamos National Laboratory, Los Alamos, New Mexico, USA

M. A. Kreslavsky, J. W. Head III, and J. F. Mustard

Brown University, Providence, Rhode Island, USA

W. V. Boynton

The University of Arizona, Tucson, Arizona, USA

Received 18 June 2002; revised 31 July 2002; accepted 12 August 2002; published 3 October 2002.

[1] Mars Odyssey Gamma-Ray Spectrometer (GRS) neutron spectrometer data are analyzed to determine the concentration and boundary of buried water ice near the south pole. The measurements are consistent with a circumpolar layer of average ice concentration from 35 to 100% by weight and superposed dust with thickness density product 30 to 40 g/cm<sup>2</sup>. The region of buried water ice extends from near the south pole to latitudes 48S to 58S. The equatorward boundary of the ice-rich region compares favorably with the boundary of an ice-rich dust mantle inferred from Mars Orbiter Laser Altimeter data and the locations of dissected terrain inferred from Mars Orbiter Camera images. The ice-rich mantle is identified as the source of enhanced hydrogen sensed by the neutron spectrometer. **INDEX TERMS:** 5462 Planetology: Solid Surface Planets: Polar regions; 5470 Planetology: Solid Surface Planets: Surface materials and properties; 5464 Planetology: Solid Surface Planets: Remote sensing. **Citation:** Tokar, R. L., W. C. Feldman, T. H. Prettyman, K. R. Moore, D. J. Lawrence, R. C. Elphic, M. A. Kreslavsky, J. W. Head III, J. F. Mustard, and W. V. Boynton, Ice concentration and distribution near the south pole of Mars: Synthesis of odyssey and global surveyor analyses, *Geophys. Res. Lett.*, 29(19), 1904, doi:10.1029/2002GL015691, 2002.

### 1. Introduction

[2] The record of variations in the climate of Mars is imprinted in the spatial distribution of a variety of structures and features of its polar deposits. Recent studies of martian south-polar terrain extending equatorward to about 50S latitude identify an ice-rich dust mantle [Kreslavsky and Head, 2002], and a ring of dissected terrain extending between about 30S and 55S latitude interpreted to be formerly ice-rich loess or dust [Mustard et al., 2001]. The location and margins of the ice-rich layer are in qualitative agreement with original Viking studies. [Farmer and Doms, 1979]. See Clifford et al. [2000] for a recent review of the state of Mars polar science.

[3] Observations from the Mars Odyssey Gamma-Ray Spectrometer (GRS) reveal enhanced abundances of hydrogen near the south pole, interpreted to be buried water ice

[Feldman et al., 2002, Boynton et al., 2002]. Similar results were obtained independently by the Russian instrument HEND onboard Odyssey [Mitrofanov et al., 2002]. These instruments sense approximately the top meter of the regolith. In this study, the analysis of the GRS neutron spectrometer data is extended to further characterize the water-ice deposits. The measurements are found to be consistent with simulations for a homogeneous circumpolar region containing water ice concentrations from 35% to 100% by weight with superposed dust having a thickness density product of 30 to 40 g/cm<sup>2</sup>. The region extends from the south pole to latitudes between 48S and 58S, and the location of the boundary compares favorably with both the equatorward boundary of the ice rich dust mantle and the poleward boundary of the dissected terrain.

### 2. GRS Neutron Spectrometer Measurements

[4] The data analyzed in this study were measured using the neutron spectrometer component of the GRS over the period 20 March to 18 April 2002, when the south Mars season is late summer and a seasonal CO<sub>2</sub> frost cover is absent. This is the same neutron data set analyzed in the Boynton et al. [2002] study, although in this paper north and south bound orbits are separated and the contributions to the counting rate from both the residual south polar cap and equatorial regions are identified. This study employs three detectors on the neutron spectrometer, one facing toward Mars and the spacecraft nadir (detector 1), one facing in the direction of the spacecraft velocity (detector 2), and one facing opposite the spacecraft velocity (detector 4). Detector 1 is covered in cadmium and is sensitive to neutrons with energies between about 0.3 eV to 600 keV. Detector 2 captures both thermal ( $E < \sim 0.3$  eV) and epithermal ( $0.3\text{eV} < E < 600$  keV) neutrons, with the thermal neutron capture enhanced by the spacecraft motion [Feldman and Drake, 1986]. The GRS neutron spectrometer is the first successful demonstration of this technique in space [Tokar et al., 2002]. Detectors 2 and 4 sample the source regions predominantly in front and behind the spacecraft, respectively. Both detectors sense neutrons from as far away as the horizon of Mars as viewed from Odyssey.

[5] Figure 1 is an overview of data measured by the neutron spectrometer as Odyssey passes over the south pole.

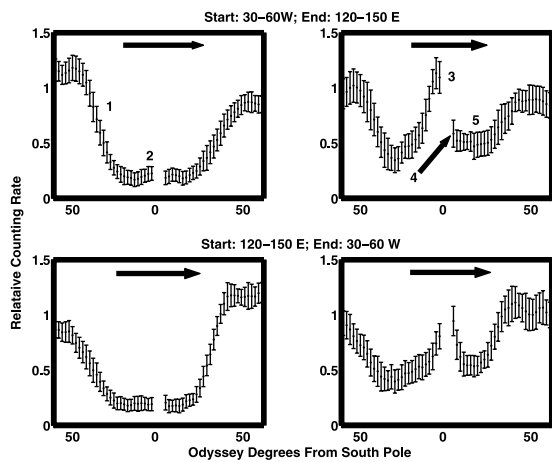


**Figure 1.** GRS neutron spectrometer data as a function of the location of the spacecraft nadir in the vicinity of the south pole. The spacecraft motion is left to right in all panels. The left column is data for the nadir pointing detector; the right column is data for the forward minus backward detectors. Point 3 is the thermal neutron signature of the residual cap and point 5 is the plateau region where the measurements are used to determine the circumpolar ice concentration.

The direction of the spacecraft motion is left to right in all panels. The data are accumulated in 2 degree latitude bins and a 30 degree longitude bin. In the top two panels, the nadir position of the spacecraft trajectories start at 30S latitude with longitudes between 30 and 60W, pass nearly over the south pole, and end at 30S and 120–150E. The bottom two panels are over the same terrain but the Odyssey orbit is in the opposite direction. The left column is neutron counting rate for the nadir-pointing cadmium-covered detector 1 relative to that measured above the Viking 1 landing site at 22N, 48W; the right column is neutron counting rate relative to the Viking site for the forward detector 2 minus the backward detector 4. At the Viking 1 site, the detector 1 counting rate is  $\sim 8.5 \text{ s}^{-1}$ , the detector 2 - detector 4 counting rate is  $\sim 7.0 \text{ s}^{-1}$ , and the water content is thought to be low,  $\sim 1\%$  by weight. The left column is an estimate of epithermal neutron flux and the right column is an estimate of thermal neutron flux, both along spacecraft trajectories. Averages and standard deviations of the counting rate samples in each latitude-longitude areal domain are shown in Figure 1 and the accumulation bins typically contain 60 measurements. All data in Figure 1 are plotted as a function of the angle of Odyssey away from the south pole.

[6] Features in the data in Figure 1 are as follows. Both panels in the left column illustrate the large dropout in the epithermal neutron flux throughout a large circumpolar region, with point 1 in the upper left denoting the steep drop in the counting rate as the region is encountered. Point 2 is a slight increase in epithermal counts attributed to the residual  $\text{CO}_2$  cap. Point 3 in the upper right panel is the large increase in thermal neutron flux also attributed to the residual  $\text{CO}_2$  cap. It should be noted that detector 2 starts to sense the cap as soon as it appears on the horizon, which is located  $\sim 25$  degrees from the nadir position. The slight upturn in count

rate at point 4 relative to the immediately succeeding points illustrates that after transiting the  $\text{CO}_2$  cap the forward detector captures thermal neutrons attributed to the cap even though the look direction of the detector is away from the cap. The velocities of these neutrons in the detector frame are directed into the detector due to the spacecraft motion. Thick solid  $\text{CO}_2$  superposed on water ice and subject to the cosmic ray flux is known to be a strong source of thermal neutrons [Drake *et al.*, 1988]. Point 5 is a plateau region in the thermal neutron flux, where the forward detector has only weak contributions from the  $\text{CO}_2$  cap behind the spacecraft and the equatorial region in front of the spacecraft. The backward looking detector registers a low counting rate in this plateau as it is directed toward the large dropout in epithermal neutron flux around the south pole. The lower right panel in the Figure is similar to the upper right, although for spacecraft motion in this opposite direction the peak in counts attributed to the residual cap is now past the pole as expected for the residual cap location. A plateau region in the neutron counting rate past the cap is observed, but it is almost immediately contaminated by neutrons that originate in the equatorial region.

### 3. Simulations

[7] The simulation developed for this study employs three surface components near the south pole. The soil compositions used are those employed in the *Feldman et al.* [2002] and *Boynton et al.* [2002] studies. Equatorward of 30–40S latitude, the soil is homogeneous and has a water content of 1% by weight. In the region surrounding the south pole and exterior to the residual cap, soil with variable water content (35–100%) is buried under dry (1% water) soil with variable depth. The residual  $\text{CO}_2$  cap is the third surface component, and it is centered on the south pole and extends 2.5 degrees off the pole. An exponentially decreasing Martian atmosphere with  $11 \text{ g/cm}^2$  thickness and 10 km scale height overlies all three source regions.

[8] In each simulation, neutron counting rates are calculated for the downward, forward, and backward looking detectors. The simulation maps accessible neutron phase space connecting source areal parcels at the top of the Martian atmosphere and each detector. The source region grid lies on the top of the atmosphere, moves with Odyssey, extends to the horizon, and is symmetric about the spacecraft nadir position. For each of  $50 \times 720$  source cells, the mapping of the accessible phase space yields neutron energies and velocity vector directions that enter the detectors. Both the Martian gravitational field and the spacecraft motion are included. The code MCNPX [Waters, 2002], with gravitational boundary conditions appropriate to Mars, is used to calculate the neutron flux as a function of energy and angle within each source cell. Following the results of *Drake et al.* [1988], the energy and angle dependence of the neutron flux produced by the  $\text{CO}_2$  cap is adjusted to yield simulated count rates in agreement with those measured by Odyssey. MCNPX is also used to calculate the response function of each neutron detector as a function of incident neutron energy and angle.

[9] Figure 2 illustrates representative simulation results as the spacecraft traverses the three component model. In this case, the surface boundaries (denoted with dotted vertical

lines) are chosen to approximate the Odyssey measurements for trajectories that enter the region at longitudes 0–30W and exit in 150–180E. The buried H<sub>2</sub>O region in this example has 40 g/cm<sup>2</sup> of 1% H<sub>2</sub>O -equivalent hydrogen material on top of soil that is 75% H<sub>2</sub>O by weight. The counting rates are normalized to the simulated equatorial region counting rates, as in Figure 1. Note that the nadir pointing detector 1 exhibits a fall off in epithermal neutron counts similar to that measured on Odyssey. In addition, the simulated forward minus backward neutron count rate exhibits many of the features observed in the data. Note the rapid increase in thermal counts as the CO<sub>2</sub> cap is approached, and the minimum in counts  $\sim$ 15 degrees past the south pole. This is a plateau region in the simulation, similar to that observed in the data, and it is located before the equatorial step at 50S enters the field of view of the forward detector. Also note that after the spacecraft nadir moves equatorward of the cap edge (located at 2.5 degrees), the forward detector is still capturing thermal neutrons that originate at the cap. This effect is observed in the data; see point 4 in Figure 1.

[10] Simulations such as the one shown in Figure 2 are performed for variable ice concentration and superposed dry-material thicknesses surrounding the pole. The focus of this study is data from the longitude band 150–180 E, although neutron measurements for all longitudes are similar. For this longitude band, the measured relative counting rates in the plateau are  $0.19 \pm 0.06$  (detector 1) and  $0.47 \pm 0.11$  (detectors 2–4). The latitude bin for the plateau is at 78S, approximately 12 degrees past the edge of the residual cap.

[11] Figure 3 summarizes the results of the simulation and data comparison. Plotted is the forward pointing (detector 2) minus backward pointing (detector 4) relative neutron counting rate versus the nadir pointing (detector 1) relative neutron counting rate. The curves are simulation results in the plateau region for the spacecraft nadir position 12 degrees past the residual cap edge and the spacecraft velocity directed northward. The measurements are consistent with 35% to 100% buried H<sub>2</sub>O underneath

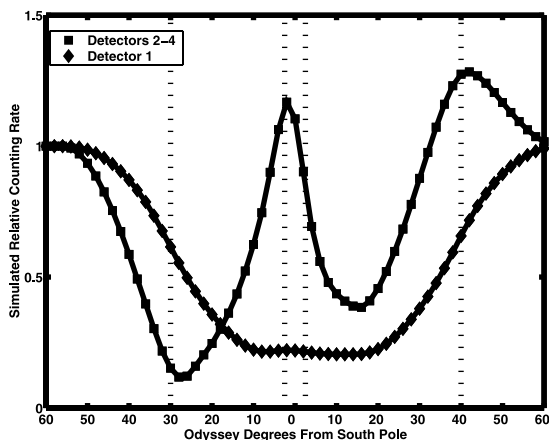


**Figure 2.** Simulated relative count rates along the Odyssey trajectory for the nadir pointing detector (1), and the forward minus backward detectors (2–4). The simulation for the simple three component source model reproduces many subtle features of the neutron measurements; compare with Figure 1.

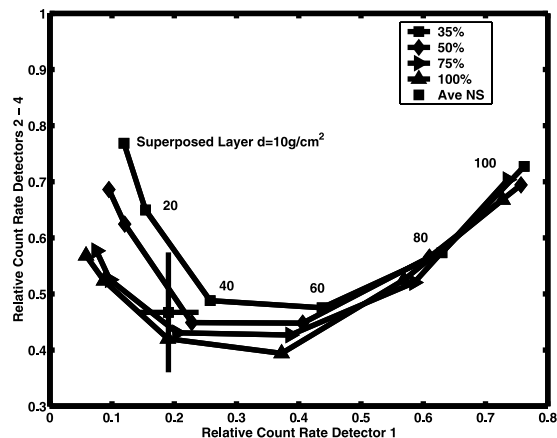


**Figure 3.** The measured relative neutron count rates for the longitude band 150–180E in the plateau are compared with simulation predictions for 35, 50, 75, and 100% buried water ice underneath a dry layer with 1% H<sub>2</sub>O by weight. The dry layer in the simulation varies in thickness density product from 10 to 100 g/cm<sup>2</sup>. The neutron data agrees with the simulation results for the buried water ice equal to 35–100% by weight, with 30 to 40 g/cm<sup>2</sup> of relatively dry material on top.

30 to 40 g/cm<sup>2</sup> of relatively dry dust. This result agrees with model results in *Boynton et al.* [2002], where the H<sub>2</sub>O content is found to be between 35% and 50%. The hydrogen gamma emission-line intensity limits the maximum amount of ice, subject to the assumptions in *Boynton et al.* [2002], to less than 50% by weight.

#### 4. Discussion

[12] Figure 4 is a map of the epithermal neutron counting rate measured by the nadir pointing neutron detector for segments of Odyssey orbits traveling south. The solid black curve is the boundary of the buried ice region obtained from the neutron data. The boundary is approximated as the nadir position of the spacecraft where the counting rate for south bound trajectories is one-half of the maximum encountered before entering the region of high water content. The black points in the Figure are the locations of dissected and eroded terrain obtained by *Mustard et al.* [2001] using Global Surveyor Mars Orbiter Camera (MOC) images. The magenta curve is the boundary of “mantled” terrain having low sub kilometer-scale roughness and a strong prevalence of concave topography. This boundary is obtained using Global Surveyor Mars Orbiter Laser Altimeter (MOLA) data as in *Kreslavsky and Head* [2002]. The boundary is difficult to determine in the region near Arygre basin (30–60W) and is omitted. A detailed discussion of previous work on this latitude-dependent mantle, including the pioneering work of *Soderblom et al.* [1973], can be found in *Kreslavsky and Head*, [2000; p. 26705–26710].

[13] *Kreslavsky and Head* [2000, 2002] used maps of the statistical characteristics of high-resolution MOLA altimetry to show the presence of a meters-thick sedimentary layer interpreted to be water-ice rich and lying poleward of about 30–50 degrees latitude. The layer is clearly relatively recent geologically (Late Amazonian), and overlies earlier

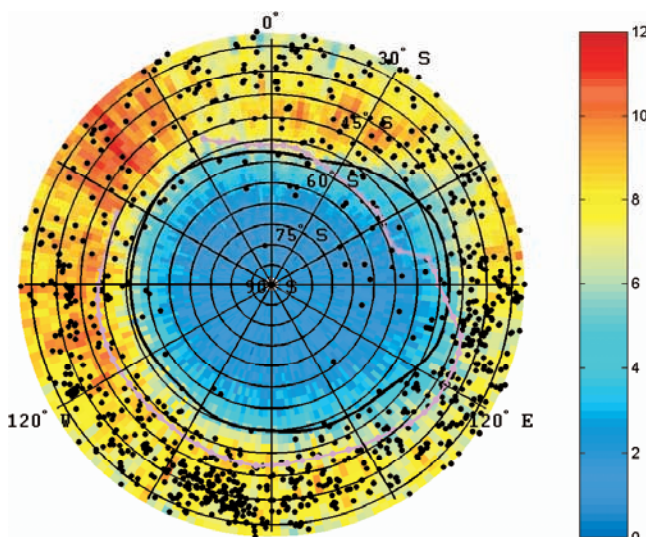


**Figure 4.** Illustrated is a map of the neutron counting rate ( $s^{-1}$ ) measured by the nadir pointing neutron detector near the south pole and for segments of Odyssey orbits directed south. The map extends to  $\sim 30S$  and the latitudinal grid lines are separated by 5 degrees. On top of the neutron data is plotted: (1) the equatorward boundary of the buried ice region determined from the neutron counting rate (black curve), (2) the dissected terrain locations identified in MOC images (black points), and (3) the poleward boundary of the ice-rich dust mantle determined with MOLA data (magenta curve).

Amazonian and older units, and the regoliths associated with these underlying units. The terrain mapped by *Mustard et al.* [2001] at latitudes between  $\sim 30\text{--}60^\circ$  was determined to be  $<150$  kyrs old and appears to be the decaying margins of the most recent episode of ice-dust mantle deposition. Within the mapped zone, ice has sublimated from the soil, equatorward of the zone, no mantle was deposited, and poleward of the zone the mantle is continuous and thus still should be ice-rich.

[14] The correspondence of these regions and margins with the concentration of near-surface water ice detected by the GRS neutron spectrometer as shown in Figure 4 is striking. For example, the boundary of the area interpreted to be characterized by the buried ice using the neutron data is about 5 degrees poleward of the line mapped as the northern boundary of the relatively continuous ice-rich mantle obtained with the MOLA data. Northward of this border lies the transitional zone with transitional roughness and no prevalence of concave topography and the regions mapped by *Mustard et al.* [2001] to be mantle deposits undergoing decay and modification. Between about 20 and 105 E, the black line reverses position with the magenta line; the maps of *Kreslavsky and Head* [2002] show this area to be characterized by a wider transitional zone at the

boundary of the continuous layer. On the basis of these correlations, the ice-rich mantle is interpreted to be the source of the water ice detected by Odyssey in the circum-polar region.

[15] **Acknowledgments.** The work at Los Alamos was performed under the auspices of the U.S. DOE and supported by the NASA Mars Odyssey program. The neutron spectrometer is a component of the University of Arizona GRS. Mars Odyssey is managed by the Jet Propulsion Laboratory for NASA.

## References

- Boynton, W. V., W. C. Feldman, S. W. Squyres, T. Prettyman, J. Bruckner, L. G. Evans, R. C. Reedy, R. Starr, J. R. Arnold, D. M. Drake, P. A. J. Englert, A. E. Metzger, I. Mitrofanov, J. I. Trombka, C. d'Uston, H. Wanke, O. Gasnault, D. K. Hamara, D. M. Jones, R. Macialis, S. Maurice, I. Mikheeva, G. J. Taylor, R. Tokar, and C. Shinohara, Distribution of hydrogen in the near-surface of Mars: Evidence for sub-surface ice deposits, *Science*, 10.1126/science.1073722, May 30, 2002.
- Clifford, S. M., et al., The state and future of Mars polar science and exploration, *Icarus*, 144, 210–242, 2000.
- Drake, D. M., W. C. Feldman, and B. M. Jakosky, Martian neutron leakage spectra, *J. Geophys. Res.*, 93(B6), 6353–6368, 1988.
- Farmer, C. B., and P. E. Doms, Global seasonal variation of water vapor on Mars and implications for permafrost, *J. Geophys. Res.*, 84(B6), 2881–2888, 1979.
- Feldman, W. C., and D. M. Drake, A Doppler filter technique to measure the hydrogen content of planetary surfaces, *Nucl. Insts. Meth. Phys. Res.*, A245, 182–190, 1986.
- Feldman, W. C., W. V. Boynton, R. L. Tokar, T. H. Prettyman, O. Gasnault, S. W. Squyres, R. C. Elphic, D. J. Lawrence, S. L. Lawson, S. Maurice, G. W. McKinney, K. R. Morre, and R. C. Reedy, Global distribution of neutrons from Mars: results from Mars Odyssey, *Science*, 10.1126/science.1073541, May 30, 2002.
- Kreslavsky, M. A., and J. W. Head III, Kilometer-scale roughness of Mars: Results from MOLA data analysis, *J. Geophys. Res.*, 105(E11), 26,695–26,711, 25 Nov 2000.
- Kreslavsky, M. A., and J. W. Head III, Mars: Nature and evolution of young latitude-dependent water-ice-rich mantle, *Geophys. Res. Lett.*, 29(15), 10.1029/2002GL015392, 2002.
- Mitrofanov, I., D. Anfimov, A. Kozyrev, M. Litvak, A. Sanin, V. Tretyakov, A. Krylov, V. Shvetson, W. Boynton, C. Shinohara, D. Hamara, and R. S. Saunders, Maps of subsurface hydrogen from the high energy neutron detector, Mars odyssey, *Science*, 10.1126/science.1073616, May 30, 2002.
- Mustard, J. F., C. D. Cooper, and M. K. Rifkin, Evidence for recent climate change on Mars from the identification of youthful near-surface ground ice, *Nature*, 412, 411–413, 26 July 2001.
- Soderblum, L., T. Kriedler, and H. Masursky, Latitudinal distribution of a debris mantle on the Martian surface, *J. Geophys. Res.*, 78, 4117–4122, 1973.
- Tokar, R. L., W. C. Feldman, T. H. Prettyman, K. R. Moore, W. V. Boynton, O. Gasnault, S. L. Lawson, D. J. Lawrence, and R. C. Elphic, Comparison of measured thermal/epithermal neutron flux and simulation predictions for the Odyssey neutron spectrometer in orbit about Mars, Proceedings, Lunar and Planetary Science Conference, Houston, TX, March 11–15, 2002.
- Waters, L. S., (ed.), “MCNPX User’s Manual, Version 2.3.0”, LA-UR-02-2607, Los Alamos National Laboratory, April 2002.

R. L. Tokar, W. C. Feldman, T. H. Prettyman, K. R. Moore, D. J. Lawrence, and R. C. Elphic, Los Alamos National Laboratory, Los Alamos, NM, USA.

M. A. Kreslavsky, J. W. Head III, and J. F. Mustard, Brown University, Providence, RI, USA.

W. V. Boynton, The University of Arizona, Tucson, AZ, USA.